Inorganic Chemistry

Article

pubs.acs.org/IC

# Water-Soluble Co(III) Complexes of Substituted Phenanthrolines with Cell Selective Anticancer Activity

Sivaraman Jagadeesan,[†,‡] Vimalkumar Balasubramanian,[⊥] Patric Baumann,[†] Markus Neuburger,[#] Daniel Häussinger,[§] and Cornelia G. Palivan*[,†]

[†]Department of Chemistry, University of Basel, Klingelbergstrasse 80, 4056, Basel, Switzerland

[‡]School of Chemistry, Bharathidasan University, Palkalaiperur, Tiruchirappalli 620 024, Tamil Nadu, India

[⊥]Department of Pharmaceutical Sciences, University of Basel, Klingelbergstrasse 50, CH-4056 Basel, Switzerland

[#]Department of Chemistry, University of Basel, Spitalstrassse 51, CH-4056 Basel, Switzerland

[§]Department of Chemistry, University of Basel, St. Johannsring 19, CH-4056 Basel, Switzerland

Supporting Information

**ABSTRACT:** Transition metal complexes with substituted phenanthrolines as ligands represent potential anticancer products without the drawbacks of platinum complexes that are currently marketed. Here, we report the synthesis and cell selective anticancer activity of five new water-soluble Co(III) complexes with methyl substituted phenanthroline ligands. The complexes were characterized by elemental analysis, NMR, FAB-mass spectrometry, FTIR, electronic spectroscopy, and single crystal X-ray diffraction. Possible interaction of these complexes with DNA was assessed by a combination of circular dichroism, UV−vis spectroscopy titration, and ethidium bromide displacement assay, and the results indicated that DNA interaction is weak for these complexes. Cellular uptake and cytotoxicity of complexes at low concentrations were assessed by flow cytometry on PC-3 cells, while their effect on intracellular mitochondrial function was measured by MTS assay on HeLa and PC-3 cell lines. These complexes showed selective cytotoxicity with a significantly higher effect on intracellular mitochondrial function in PC-3 cells than in HeLa cells. At low concentrations, complex **2** had the highest cytotoxic effect on PC-3 cells, inducing around 38% cell death, and the correlation of cytotoxicity of these complexes to their hydrophobicity indicates that an appropriate value of the hydrophobicity is essential for high antitumor activity.

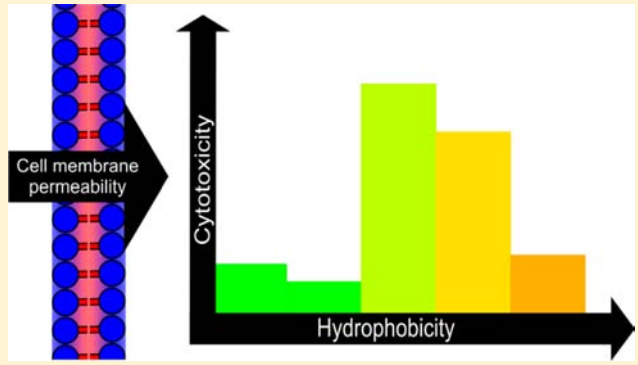


## INTRODUCTION

Chemotherapy with metal complexes is an effective approach for fighting cancer, and Pt-complexes, such as *cis*-diamminedichloroplatinum(II) (CDDP), carboplatin and oxaliplatin, are already on the market.[1,2] The cytotoxicity of these metal complexes has been attributed to interactions with cellular targets, as for example binding to GpG DNA sequences, inducing a disruption of the cellular transcription,[3−5] and interaction with mitochondrial DNA and proteins.[6,7] However, these Pt complexes are associated with serious side effects, such as nephro-, gastrointestinal, and hematological toxicity, and recently, it has been reported that tumor cells can develop resistance against them.[8−10] Intensive efforts have been made to develop new metal complexes that are effective against cancer cells either by changing the metal or the ligand type. Various transition metals combined with a variety of ligand classes, such as Schiff bases, amino acids, and extended polypyridine have been proposed to improve the efficacy of cancer treatment,[11−16] but many proposed complexes have either shown poor selectivity against specific cancer cells or failed to pass clinical trials due to a poor solubility in water.[17,18] However, ligands based on phenanthroline derivatives have attracted interest, because associated metal complexes have been reported to be active against various pathologic conditions including cancer, microbial, and fungal infections.[19,20] Furthermore, transition metal complexes containing substituted phenanthroline ligands have higher cytotoxicity than CDDP on cancer cell lines, and thus understanding their interaction with DNA has attracted particular attention.[21−25]

Cobalt is an essential element present in biological systems either as metal center in vitamin $B_{12}$ and other cobalamines or as an ion involved in cellular oxidative stress through mitochondrial mediated apoptosis.[26] The involvement of Co ions in oxidative stress and the interaction of Co(III/II) complexes with DNA are important factors that explain their high cytotoxicity and support their further development as potential anticancer drugs.

**Received:** June 26, 2013
**Published:** October 15, 2013

   dx.doi.org/10.1021/ic4016228 | *Inorg. Chem.* 2013, 52, 12535−12544

Here we present the synthesis and cytotoxic activity of five new water-soluble cobalt(III) complexes with ligands of the type $[Co(N{-}N)_2Cl_2]Cl$, where N−N = 5,6-dimethyl-1,10-phenanthroline (5,6-dmp) (**1**), 4,7-dimethyl-1,10-phenanthroline (4,7-dmp) (**2**), 3,4,7,8-tetramethyl-1,10-phenanthroline (tmp) (**3**), 5-methyl-1,10-phenanthroline (5-mp) (**4**), and 4-methyl-1,10-phenanthroline (4-mp) (**5**). The structures of the complexes were determined by elemental analysis, NMR, FAB-MS, IR and electronic spectroscopy. In addition, the structure of complexes **1**, **2**, and **3** was refined by single crystal X-ray diffraction. In order to determine the possible interaction of these complexes with DNA, a combination of circular dichroism (CD), UV−vis spectroscopy titration, and ethidium bromide (EthBr) displacement assay was used. Cytotoxicity was assessed on HeLa and PC-3 cancer cell lines by MTS assay and flow cytometry. Interestingly, high cytotoxicity was found to be related to specific hydrophobicity, rather than to strong DNA interaction, a result that gives a new insight into the relevance of physical properties and interactions of Co complexes proposed as anticancer agents.

## EXPERIMENTAL SECTION

**Materials and Methods.** All chemicals were purchased from Sigma Aldrich and Alfa Aesar and used without further purification. Calf thymus DNA (CT-DNA) was obtained from Sigma Aldrich.

*NMR.* $^1$H, $^{13}$C NMR, and 2D NMR measurements were carried out in DMSO-$d_6$ solutions on Bruker Avance III spectrometers, operating at either 400 or 600 MHz, and equipped with self-shielded *z*-axis pulsed field gradient dual broadband direct observation probe-heads. Chemical shifts were referenced to residual solvent peaks, and the temperature was calibrated using a methanol sample. ROESY experiments were performed with 2048 time points in F2 and 512 time increments in the indirect dimension F1, which corresponds to acquisition times of 170 ms in F2 and 43 ms in F1. Mixing times were 0.2 s. For each increment, eight scans were recorded, requiring a total experiment time of 2.2 h.

*UV−vis Spectroscopy.* Absorption measurements (200−800 nm) on all of the complexes in PBS buffer solutions were performed at room temperature using an Analytikjena UV-Specord 210 plus (edition 2010) UV−visible spectrophotometer.

*FTIR Spectroscopy.* Infrared spectra between 400 and 4000 cm$^{-1}$ were obtained at room temperature with a resolution of 1 cm$^{-1}$ using a Bruker-alpha spectrometer.

*Fast Atom Bombardment Mass Spectrometry, FAB-MS.* FAB-MS measurements were performed with a Finnigan MAT model-8430 mass spectrometer at room temperature. Complexes **1**−**5** were dissolved in nitrobenzene alcohol (NBA), and the mass scan range was from 35 to 1500 amu.

Microanalysis (C, H, and N) was performed with a vario MICRO CUBE elemental analyzer.

*Circular Dichroism, CD.* CD spectra were obtained with an AVIV circular dichorism spectrometer model 62ADS at 25 °C using a 0.1 mm path length quartz cell.

**Preparation of Complexes.** All of the complexes, *cis*-$[Co(5,6\text{-dmp})_2Cl_2]Cl$ (**1**), $[Co(4,7\text{-dmp})_2Cl_2]Cl$ (**2**), $[Co(tmp)_2Cl_2]Cl$ (**3**), $[Co(5\text{-mp})_2Cl_2]Cl$ (**4**), and $[Co(4\text{-mp})_2Cl_2]Cl$ (**5**), where 5,6-dmp = 5,6-dimethyl-1,10-phenanthroline, 4,7-dmp = 4,7-dimethyl-1,10-phenanthroline, tmp = 3,4,7,8-tetramethyl-1,10-phenanthroline, 5-mp = 5-methyl-1,10-phenanthroline, and 4-mp = 4-methyl-1,10-phenanthroline, were synthesized by a slight modification of the procedure described by Gosh et al.[27] Methanolic solutions of ligands (2 equiv) were refluxed for 1 h before addition of anhydrous cobalt chloride (1 equiv) in 10 mL of methanol. The mixture color, which changed from yellow to dark brown, was cooled in ice, and chlorine gas was passed through it. The resulting precipitate was dissolved in 50 mL of 0.001 M hydrochloric acid by warming to 60 °C for 30 min. Then after the solution was cooled to 25 °C, 20 mL of 4 M hydrochloric acid was added, and the resulting mixture was kept overnight. The resulting precipitates were filtered, washed with an excess of ethyl acetate, and dried in a vacuum.

*cis-[Co(5,6-dmp)$_2$Cl$_2$]Cl (**1**).* $^1$H NMR: (ppm, 400 MHz, DMSO-$d_6$, 25 °C) 10.06 (d, $J$ = 5.0 Hz, 2H), 9.42 (d, $J$ = 8.0 Hz, 2H), 8.89 (d, $J$ = 8.2 Hz, 2H), 8.56 (dd, $J$ = 8.5, 5.4 Hz, 2H), 7.62 (dd, $J$ = 8.4, 5.4 Hz, 2H), 7.43 (d, $J$ = 5.3 Hz, 2H), 2.95 (s, 6H), 2.80 (s, 6H). $^{13}$C NMR: (ppm, DMSO-$d_6$, 25 °C) 153.58, 150.34, 146.82, 145.51, 137.66, 136.82, 132.79, 132.55, 131.30, 130.71, 127.50, 126.86, 15.21, 15.00. UV−vis: (PBS-buffer, nm) ($\varepsilon$, M$^{-1}$ cm$^{-1}$): 520 (80.46), 283 (44,580). IR (cm$^{-1}$): 448 $\upsilon$ (Co−N); 819 $\upsilon$ (5,6-dmp). FAB Mass (NBA, $m/z$): 545.1 $[Co(5,6\text{-dmp})_2Cl_2]^+$, Anal. Calcd. for $C_{28}H_{24}Cl_3CoN_4.3H_2O$: C, 52.89; H, 4.76; N, 8.81. Found: C, 52.76; H, 4.90; N, 8.55.

*cis-[Co(4,7-dmp)$_2$Cl$_2$]Cl (**2**).* $^1$H NMR (ppm, 400 MHz, DMSO-$d_6$, 25 °C) 9.92 (d, $J$ = 5.6 Hz, 2H), 8.60 (d, $J$ = 9.3 Hz, 2H), 8.43 (d, $J$ = 9.0 Hz, 4H), 7.48 (d, $J$ = 5.7 Hz, 2H), 7.36 (d, $J$ = 5.6 Hz, 2H), 3.20 (s, 6H), 2.85 (s, 6H). $^{13}$C NMR: (ppm, DMSO-$d_6$, 25 °C) 154.05, 151.04, 150.81, 150.38, 147.38, 145.96, 130.52, 129.98, 128.28, 127.55, 124.87, 124.62, 18.59, 18.02. UV−vis: (PBS buffer, nm) ($\varepsilon$, M$^{-1}$ cm$^{-1}$): 519 (85.46), 273 (62,420). IR (cm$^{-1}$): 441 $\upsilon$(Co−N); 870, 852 (4,7-dmp). FAB Mass (NBA, $m/z$): 545.1 $[Co(4,7\text{-dmp})_2Cl_2]^+$, Anal. Calcd. for $C_{28}H_{24}Cl_3CoN_4.3H_2O$: C, 52.89; H, 4.76; N, 8.81. Found: C, 53.20; H, 4.95; N, 8.61.

*cis-[Co(tmp)$_2$Cl$_2$]Cl (**3**).* $^1$H NMR (ppm, 400 MHz, DMSO-$d_6$, 25 °C) 9.73 (s, 2H), 8.62 (d, $J$ = 9.4 Hz, 2H), 8.45 (d, $J$ = 9.4 Hz, 2H), 7.14 (s, 2H), 3.08 (s, 6H), 2.84 (s, 6H), 2.73 (s, 6H), 2.18 (s, 6H). $^{13}$C NMR: (ppm, DMSO-$d_6$, 25 °C) 154.24, 150.70, 148.57, 148.11, 146.71, 145.29, 136.32, 135.92, 129.57, 128.98, 124.71, 124.22, 18.40, 17.60, 14.98, 14.46. UV−vis: (PBS buffer, nm) ($\varepsilon$, M$^{-1}$ cm$^{-1}$): 523 (84.74), 280 (62,960). IR (cm$^{-1}$): 485 $\upsilon$(Co−N); 825, 816 (tmp). FAB mass (NBA, $m/z$): 601.1 $[Co(tmp)_2Cl_2]^+$, Anal. Calcd. for $C_{32}H_{32}Cl_3CoN_4{\cdot}3H_2O$; C, 55.54; H, 5.54; N, 8.10. Found: C, 55.52; H, 5.65; N, 7.98.

*cis-[Co(5-mp)$_2$Cl$_2$]Cl (**4**).* Three different isomers of complex **4** were formed as a statistical mixture as demonstrated by NMR experiments. UV−vis (PBS buffer, nm) ($\varepsilon$, M$^{-1}$ cm$^{-1}$): 518 (70.00), 278 (53,540). IR (cm$^{-1}$): 438 $\upsilon$(Co−N); 877, 803 (5-mp). FAB Mass (NBA, $m/z$): 517 $[Co(5\text{-mp})_2Cl_2]^+$, Anal. Calcd. for $C_{26}H_{20}Cl_3CoN_4{\cdot}3H_2O$: C, 51.38; H, 4.31; N, 9.22. Found: C, 51.13; H, 4.58; N, 9.27.

*cis-[Co(4-mp)$_2$Cl$_2$]Cl (**5**).* Three different isomers of complex **5** were formed as a statistical mixture as demonstrated by NMR. UV−vis (PBS buffer, nm) ($\varepsilon$, M$^{-1}$ cm$^{-1}$): 523 (85.78), 273 (57,000). IR(cm$^{-1}$): 448 $\upsilon$(Co−N); 838, 764 (4-mp). FAB Mass (NBA, $m/z$): 517 $[Co(4\text{-mp})_2Cl_2]^+$, Anal. Calcd. for $C_{26}H_{20}Cl_3CoN_4{\cdot}2H_2O$: C, 52.95; H, 4.10; N, 9.50. Found: C, 53.16; H, 4.44; N, 9.48.

**Crystal Structure Determination.** Single crystals of complexes **1**−**3** were measured on a Bruker Kappa Apex2 diffractometer at 123 K using graphite-monochromated Mo K$\alpha$-radiation with $\lambda$ = 0.71073 Å. The Apex2 suite was used for data collection and integration. The structures were solved by direct methods using the program SIR92,[28] and least-squares refinements against F were carried out on all non-hydrogen atoms. Chebychev polynomial weights were used to complete the refinement. Ellipsoid plots were drawn using Ortep-3 for Windows,[29] and Mercury versions 2.3 and 2.4[30] were used to analyze the structures. Data collection and refinement parameters are listed in Supporting Information (Table S1), and selected bond distances and angles are given in Supporting Information (Table S2). Single crystals were grown by slow evaporation at room temperature using methanol−chloroform (1:1) for complexes **1** and **2**, and acetone−acetonitrile (1:1) for complex **3**.

**Binding of Co Complexes to DNA.** To determine the interactions between Co-complexes and DNA, a combination of UV−vis spectroscopy titration, fluorescence quenching, CD, and partition coefficient determination was used.

*UV−vis Spectroscopy.* Stocks solutions of complexes (**1**−**5**) were prepared by dissolving them in 5 mM Tris-HCl/50 mM NaCl buffer at pH 7.1. The concentration of DNA per nucleotide was determined by UV−vis spectroscopy using the molar absorption coefficient (6600 M$^{-1}$ cm$^{-1}$) at 260 nm.[27] Titrations were performed by dissolving an appropriate amount of metal complex in CT-DNA solutions of


dx.doi.org/10.1021/ic4016228 | Inorg. Chem. 2013, 52, 12535−12544

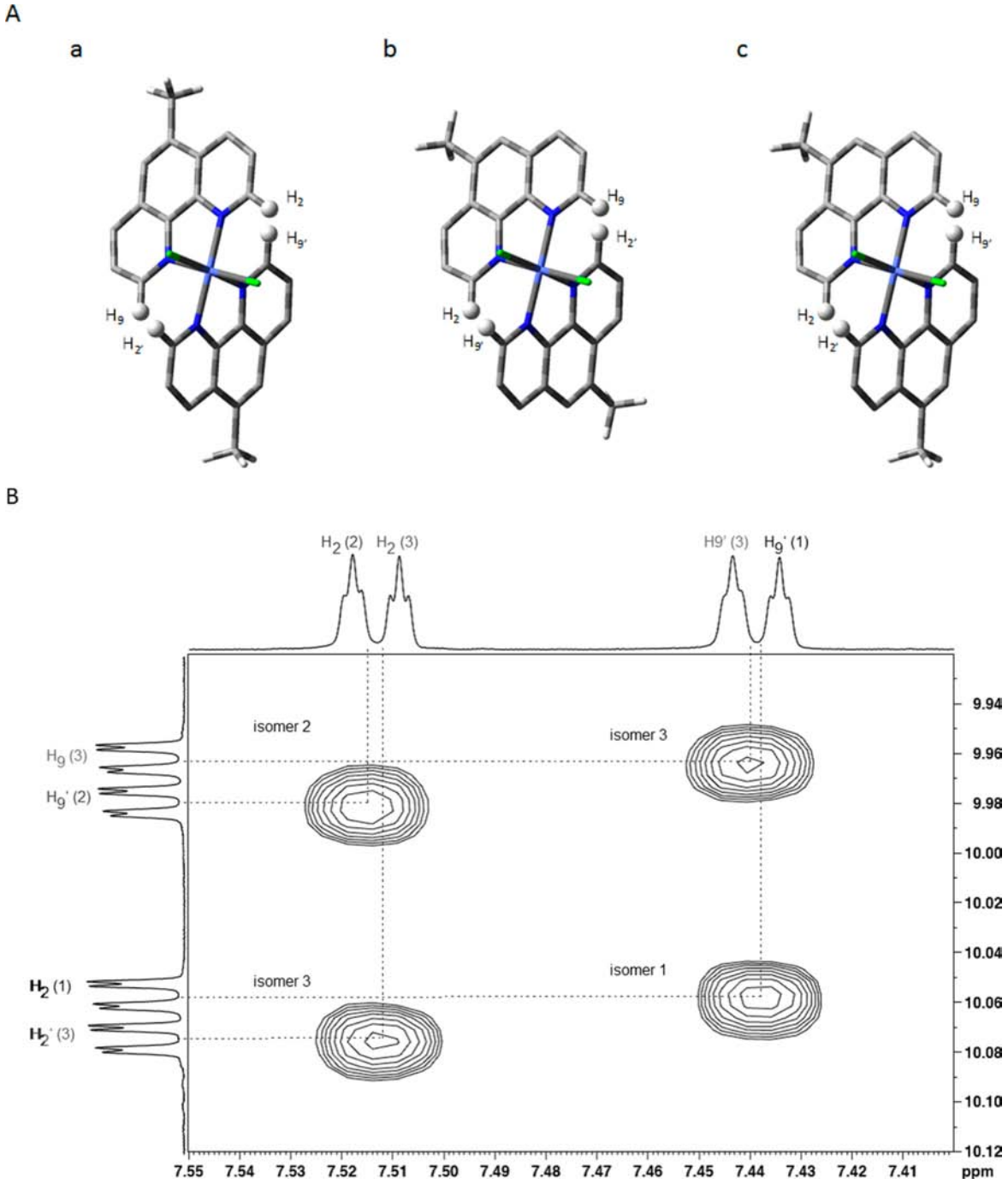


**Figure 1.** (A) Statistical mixture of isomers for complex **4**: (a) isomer 1 (trans $N_1$–$N_{1'}$), (b) isomer 2 (trans $N_{10}$–$N_{10'}$), and (c) isomer 3 (trans $N_{10}$-$N_{1'}$), and (B) ROESY spectrum of the isomers of complex **4**, in DMSO-$d_6$, at 298 K, and $\nu$ = 600 MHz.

increasing concentrations and maintaining a constant total volume. A series of Co-complexes and CT-DNA mixtures with constant concentration of metal complex and increasing concentration of CT-DNA were prepared, and the intensity of the absorption spectra at wavelengths 283, 273, 280, 278, and 273 nm was used to assess the interaction between CT-DNA and complexes **1**–**5**.

*Fluorescence Spectroscopy.* For fluorescence quenching experiments, CT-DNA was pretreated with ethidium bromide (EthBr) (1:1) for 0.5 h, and the mixture was excited at 450 nm. Emission was observed in the domain of wavelengths between 500 and 700 nm. Metal complexes were added to the CT-DNA–EthBr mixture, and the emission intensity was measured at $\lambda$ = 595 nm.

*Circular Dichroism.* CD spectra of CT-DNA and mixtures of CT-DNA with Co complexes were obtained in Tris-HCl buffer using 0.1 mm quartz cells. Each CD spectrum was obtained as an average of at least three scans, and background correction was performed for each spectrum.

*Partition Coefficients Determination.* Complexes **1**–**5** were dissolved in a mixture of PBS buffer and *n*-octanol. The mixture was shaken for 1 h, and a phase separation resulted.[31] The concentration of metal complexes in *n*-octanol and PBS buffer was determined by electronic spectroscopy at room temperature, and the formula for log P values is included in Supporting Information.

**Cell Culture.** Both PC-3 and HeLa cells were kept in Dulbecco's Modified Eagle's medium (DMEM) supplemented with 10% fetal calf serum, 1% penicillin (10 000 units $mL^{-1}$), streptomycin (10 000 $\mu$g $mL^{-1}$), 2 mM L-glutamine, and 1 mM pyruvate. Cells were grown in a humidified incubator at 37 °C in a 5% $CO_2$ atmosphere.


dx.doi.org/10.1021/ic4016228 | *Inorg. Chem.* 2013, 52, 12535–12544

Cytotoxicity of Co complexes was assessed with a combination of MTS assay and flow cytometry.

*MTS Assay.* The MTS (3-(4,5-dimethylthiazol-2-yl)-5-(3-carboxymethoxyphenyl)-2-(4-sulfophenyl)-2H-tetrazolium) assay was performed as described previously.[32] Cells were cultured in a 96-well plate, at a density of $1 \times 10^4$ cells per well, in 100 $\mu$L of DMEM medium per well for 24 h. The DMEM medium was then replaced with a mixture of fresh medium and 20 $\mu$L of Co complexes with different concentrations, and incubated for 24 h. Finally each well was refilled with fresh medium and 20 $\mu$L of aqueous solution of cell proliferation MTS reagent and incubated for 2 h. The OD of each well was measured with a Spectromax M5e microplate reader at $\lambda$ = 490 nm.

*Flow Cytometry.* For flow-cytometry analysis, PC cells at a density of $1 \times 10^5$ were cultured in 12-well plates and allowed to adhere for overnight. Cells were then treated with complexes **1**−**5**, at a concentration of 2.5 $\mu$M for 24 h at 37 °C followed by propidium iodide (1 $\mu$g/mL) staining for 30 min. Then, cells were washed with PBS to remove the unbound metal complexes and trypsinized while in the proliferative stage. Collected cells were analyzed for uptake of the metal complexes with a FSC diode detector and SSC photomultiplier detector. Cytotoxicity relevant to the DNA was measured in the FL-2 channel (CYAN, Beckman Coulter). A total of 20 000 events were analyzed for each condition.

## RESULTS AND DISCUSSION

**Co-Complexes Characterization.** All Co complexes (**1**−**5**) were prepared according to a slightly modified procedure of the method reported by Gosh et al.[27] and characterized by a combination of elemental analysis, FT-IR spectroscopy, electronic spectroscopy, NMR, and FAB mass spectrometry. In addition, the structures of complexes **1**−**3** were refined by single crystal X-ray diffraction. Elemental analyses indicated that all complexes are mononuclear, with two ligand molecules per metal ion.

FT-IR spectroscopy was used to determine the mode of coordination of the ligand to the metal. In each of the complexes coordination to the metal ion resulted in a shift in the values of $\delta$ (C−H) corresponding to the ligands (around 850 $cm^{-1}$, 740 $cm^{-1}$), and the ring (at around 1560 $cm^{-1}$), to around 840 $cm^{-1}$, 720 $cm^{-1}$, and 1500 $cm^{-1}$, respectively. The appearance of $\delta$ (Co−N) at around 440 $cm^{-1}$ indicates that the ligands coordinate to the metal through nitrogen atoms.[27,33]

The electronic spectra of the complexes are characterized by ligand-based transitions ($\lambda$ = 273−283 nm), and d−d transitions ($\lambda$ between 518 and 523 nm), in agreement with the reported bands for polypyridyl-Co(III) complexes with octahedral geometry around the metal.[27]

$^1$H- and $^{13}$C-{$^1$H}-NMR spectra of complexes **1**−**3** unambiguously demonstrate a single conformation with C2-symmetry, but complexes **4** and **5** contain a statistical mixture of three isomers as a result of the low symmetry of the ligands (Figure 1A for complex **4**, Supporting Information Figure S1 for complex **5**). Full characterization of all six isomers was achieved by 2D-NMR methods including COSY, long-range COSY, HMQC, HMBC, and ROESY experiments for complex **4** (Figure 1B) and **5** (Supporting Information Figure S2). Aromatic protons appear in the region $\delta$ = 7−10 ppm, whereas the methyl protons appear in the region $\delta$ = 2−3.5 ppm (Supporting Information Figures S3−S12). A detailed assignment of all proton and carbon atoms in complexes **4** and **5** is given in Supporting Information (Table S3 and S4).

FAB-MS spectra of all of the Co complexes dissolved in a nitrobenzene alcohol matrix showed molecular ion peaks at 545.1, 545.1, 601.1, 517.0, and 517.0. The isotopic pattern of complexes **1**−**5** is attributed to hexacoordinated cationic complexes with two ligands and two chlorine atoms attached to the cobalt atom (Supporting Information Figures S13−S17).

**Crystal Structure of Co Complexes.** The data sets obtained from crystals of Co complexes **1**−**3** with chlorine as counterion did not produce satisfactory refinements; thus new complexes were synthesized $NH_4PF_6$ instead of chlorine. Comparison of the preliminarily results on crystals of the Cl containing complexes with the final coordinates obtained on crystals with $PF_6$ indicated no significant geometrical difference. The crystallographic details are summarized for complexes **1**−**3** in Supporting Information (Table S1). Selected interatomic distances and angles for the cobalt complexes are presented in the Supporting Information (Table S2), and the molecular structures of the complexes are presented in Figures 2−4. In

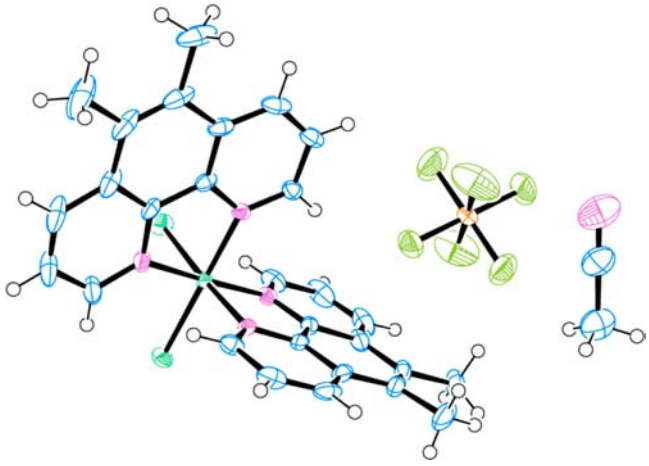

**Figure 2.** ORTEP representation of the X-ray crystal structure of **1** with 50% thermal ellipsoids.

the crystal structure of complex **1**, cobalt is hexacoordinated with a distorted octahedral geometry consisting of four N donors from the two 5,6-dimethyl-1,10-phenanthroline ligands, which are perpendicular to each other. The remaining two positions are occupied by unidentate Cl ions in cis configuration. Even though the coordination geometry gives the possibility of *C*2 symmetry with a rotation axis, the Co atom is not located on this symmetry element. One $PF_6$ as counterion and one molecule of methanol as solvent of crystallization were found in the molecular structure of complex **1** when Cl ion was replaced by $PF_6$. The Cl(1)−Cl(2) bite distance was 3.245 (1) Å, which is within the average range observed in bis(diimine)-Co(III) complexes.[27]

The crystal structure of complex **2** is similar to that of complex **1**, the only difference being the chemical nature of the ligand. There is one $PF_6$ counterion per complex molecule, and both are located on 2-fold axes of the space group *C*2/*c*. However, the methanol molecule is disordered, and SQUEEZE was used for the final refinement. The Cl(1)−Cl(2) bite distance of 3.191 (2) Å, obtained using the symmetry operation $(-x + 1, y, -z + 3/2)$, is within the average range observed in bis(diimine) Co(III) complexes.[27]

Complex **3** also has a similar structure to complexes **1** and **2**, the only difference being replacement of one chlorine atom during crystallization by a molecule of acetonitrile and balancing the charge by two $PF_6$ counterions present in the asymmetric unit.


dx.doi.org/10.1021/ic4016228 | *Inorg. Chem.* 2013, 52, 12535−12544

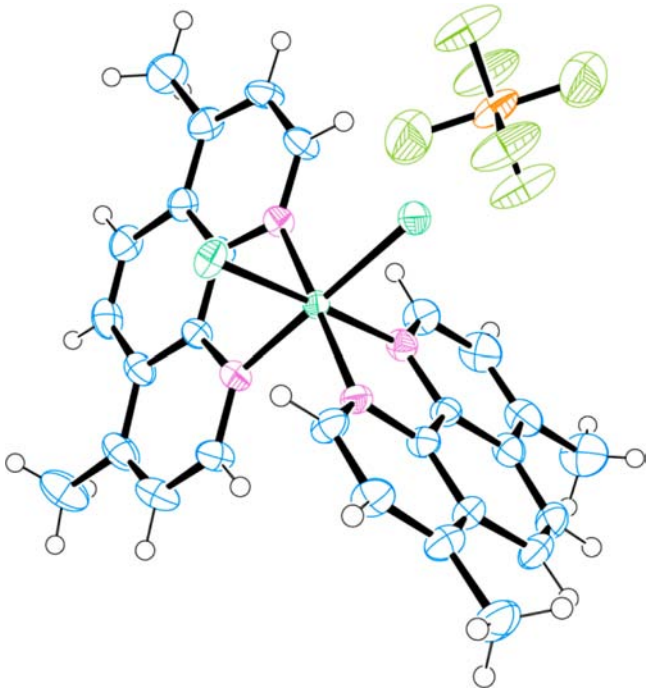

**Figure 3.** ORTEP representation of the X-ray crystal structure of **2** with 50% thermal ellipsoids.

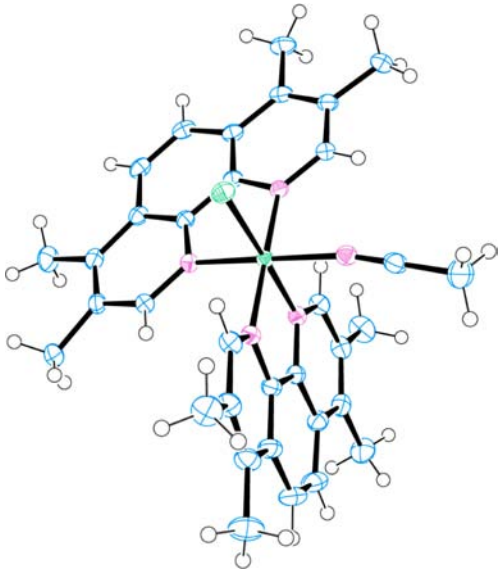

**Figure 4.** ORTEP representation of the X-ray crystal structure of **3** with 50% thermal ellipsoids. Solvent and counterions are omitted for clarity.

The mean values for the Co−N bond length in complexes **1**, **2**, and **3** are 1.9409(18) Å, 1.9385(3) Å, and 1.9351(15) Å, respectively, and the corresponding mean Co−Cl bond lengths are 2.2123 (6) Å, 2.2310(11) Å, 2.2284 (5) Å, respectively. These values are in agreement with the bond lengths obtained for the unsubstituted phenanthroline Co(III) complex.[27]

**DNA Binding by Co-Complexes.** Upon addition of CT-DNA to complexes **1**−**5**, the ligand-based spectral bands ($\pi \rightarrow \pi^*$) indicated hypochromism with very small red shifts (Figure 5). The spectra of complexes **2**, **3**, and **5** show a red shift of 4 nm, which is similar to that observed in the unsubstituted phenanthroline Co(II)-complex.[23]

Complexes **1** and **4**, which are structurally similar, show a very small shift of <2 nm, and this is attributed to the hydrophobic interaction of the methyl groups of the phenanthroline ligands with DNA via groove binding.[34] The values calculated for the binding constant, $K_b$, of these complexes (Supporting Information) are presented together with values reported for other metal complexes that have been proposed for use as anticancer compounds (Table 1).

Complexes **1** and **3** have slightly higher binding constants than complexes **2** and **4**, because the interaction with DNA is favored by the methyl groups present in the 5,6-position of the phenanthroline (complex **1**) or by a higher number of methyl groups (complex **3**).[24] However, compared to other metal complexes with similar ligands already proposed as anticancer agents because of their interactions with DNA, our complexes have lower $K_b$ values (Table 1). Thus in our Co complexes, the weak binding to DNA is not expected to play a key role in their biological activity.

As our complexes are nonfluorescent, we performed an ethidium bromide (EthBr) displacement assay to obtain more information on the competitive DNA binding of our complexes.[35] The emission intensity of EthBr, enhanced by its strong stacking interaction between adjacent DNA base pairs, is expected to decrease upon addition of molecules competing with EthBr for DNA binding, and the extent of quenching the DNA-bound EthBr emission is used to assess the binding of a second molecule to DNA. The emission intensity of DNA-bound EthBr is decreased by either replacing the DNA-bound EthBr (if the molecule binds stronger than EthBr) and/or by accepting the excited state electron from EthBr.[35] Complexes **1**−**5** all induced a moderate decrease of the emission intensity of DNA-bound EthBr (Figure 6) compared with complexes reported as strongly interacting with DNA.[22] Therefore they did not compete efficiently with the strong intercalator EthBr; thus we can rule out complete EthBr displacement with these complexes.

The values of the apparent DNA binding constant ($K_{app}$) calculated for these complexes (Supporting Information Table S5) are significantly lower than the ones of other metal complexes with high DNA binging affinity, which contain phenanthroline ligands ($1.5 \times 10^6$ $M^{-1}$ and $0.6 \times 10^6$ $M^{-1}$).[22] The values of the apparent DNA binding constants indicate in the case of our complexes a weak interaction with DNA, in agreement with the low $K_b$ values we obtained.

Circular dichroism was used to investigate possible conformational changes in DNA in the presence of complexes **1**−**5**. Solutions of CT-DNA ($7 \times 10^{-5}$ M) show a positive band at 276 nm due to the DNA base stacking and a negative band at 247 nm due to the helicity of the right-handed DNA.[35] Only complex **1** altered the helicity and base stacking of DNA (Figure 7), as indicated by the appearance of new negative bands at 233 and 295 nm and hyperchromism in the base stacking of DNA. A similar biphasic CD signal was observed for iron complexes containing 5,6-dmp ligands when interacted with CT-DNA via exciton coupling between the 5,6-dmp ligand of DNA-bound and unbound complexes.[22] Complexes **2**−**5** did not alter the DNA conformation. CD spectra revealed that the presence of methyl groups in positions 5 and 6 of the phenanthroline ligands induces changes in DNA conformation, while their presence in other positions does not.

Another factor that has been considered as important in anticancer activity of metal complexes is their hydrophobicity.[4,31] This was investigated by the partition coefficient, P a


dx.doi.org/10.1021/ic4016228 | Inorg. Chem. 2013, 52, 12535−12544

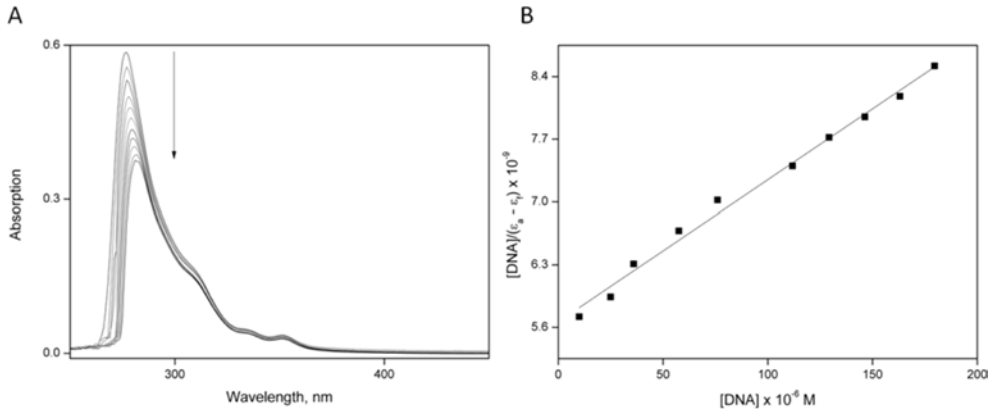


**Figure 5.** (A) Absorption spectra of complex **2** ($10 \times 10^{-6}$ M) in 5 mM Tris-HCl/50 mM NaCl buffer at pH 7.1 without addition of DNA, and by addition of increasing amounts of DNA ($R$ = [DNA]/[complex] = 1−20). (B) Dependence of the ratio [DNA]/($\varepsilon_a - \varepsilon_f$) as function of DNA concentration for complex **2**.

**Table 1. Ligand-Based Absorption Spectral Properties of Complexes 1−5 in the Presence of Increasing Amounts of CT-DNA**

| complex | $\lambda$-max [nm] | change | red shift [nm] | $K_b$, $M^{-1}$ | ref |
|---|---|---|---|---|---|
| $[Co(5,6\text{-dmp})_2Cl_2]Cl$ (**1**) | 283 | hypochromism | 1 | $3.39 \pm 0.06 \times 10^3$ | present work |
| $[Co(4,7\text{-dmp})_2Cl_2]Cl$ (**2**) | 273 | hypochromism | 4 | $2.49 \pm 0.03 \times 10^3$ | present work |
| $[Co(tmp)_2Cl_2]Cl$ (**3**) | 280 | hypochromism | 4 | $3.44 \pm 0.12 \times 10^3$ | present work |
| $[Co(5\text{-mp})_2Cl_2]Cl$ (**4**) | 278 | hypochromism | 2 | $1.98 \pm 0.11 \times 10^3$ | present work |
| $[Co(4\text{-mp})_2Cl_2]Cl$ (**5**) | 273 | hypochromism | 4 | $3.14 \pm 0.06 \times 10^3$ | present work |
| $[Cu(phen)_3]^{2+}$ | 270 | hypochromism | 6 | $9.80 \pm 0.12 \times 10^3$ | 35 |
| $[Cu(5,6\text{-dmp})_3]^{2+}$ | 280 | hypochromism | 2 | $3.80 \pm 0.05 \times 10^4$ | 35 |
| $[Zn(phen)_3]^{2+}$ | 267 | hypochromism | 14 | $3.40 \pm 0.16 \times 10^4$ | 35 |
| $[Zn(5,6\text{-dmp})_3]^{2+}$ | 278 | hypochromism | 2 | $3.07 \times 10^4$ | 35 |
| $[Rh(phen)_2]^{+}$ | | | | $1.5 \times 10^2$ | 11 |
| $[Fe(phen)_3]^{2+}$ | 267 | hypochromism | 4 | $6.8 \pm 0.1 \times 10^3$ | 22 |
| $[Fe(5,6\text{-dmp})_3]^{2+}$ | 278 | hypochromism | 0 | $4.8 \pm 0.1 \times 10^3$ | 22 |
| $[Co(phen)_3]^{2+}$ | 270 | hypochromism | 4 | $7.2 \pm 0.09 \times 10^3$ | 23 |
| $[Co(5,6\text{-dmp})_3]^{2+}$ | 280 | hypochromism | 0 | $2.80 \pm 0.05 \times 10^4$ | 23 |
| $[Ni(phen)_3]^{2+}$ | 267 | hypochromism | 6 | $1.40 \pm 0.16 \times 10^4$ | 23 |
| $[Ni(5,6\text{-dmp})_3]^{2+}$ | 278 | hypochromism | 0 | $3.17 \pm 0.07 \times 10^4$ | 23 |
| $[Cu(tdp)(tmp)]^{+}$ | 269 | hypochromism | 1 | $7.0 \pm 0.2 \times 10^5$ | 24 |

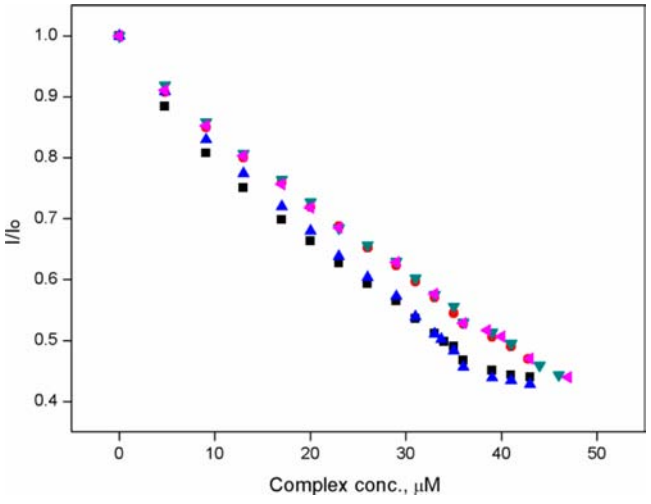


**Figure 6.** Effect of addition of complexes **1**−**5** (black squares for complex **1**, red circles for complex **2**, blue triangles for complex **3**, green triangles for complex **4**, and pink triangles for complex **5**) on the emission intensity of the CT-DNA−EthBr complex at different complex concentrations ($0-50 \times 10^{-6}$ M). [EthBr] = $10 \times 10^{-6}$ M, [CT-DNA] = $10 \times 10^{-6}$ M.

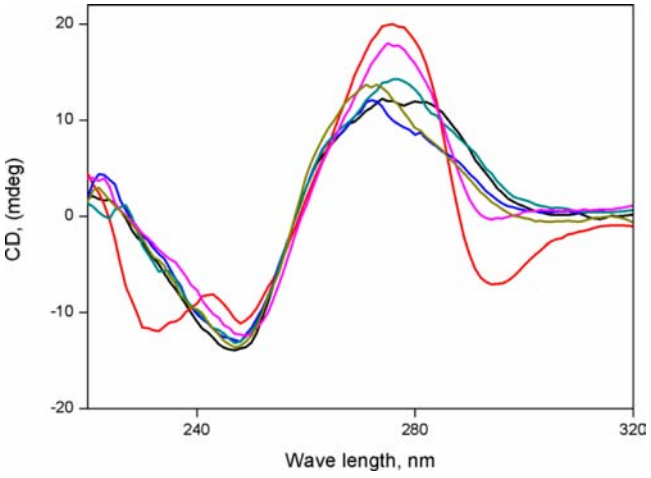


**Figure 7.** Circular dichroism spectra of CT-DNA: without (black curve) and in the presence of complexes **1**−**5** (red line for complex **1**, blue line for complex **2**, blue-green line for complex **3**, pink line for complex **4**, and green line for complex **5**). [CT-DNA] = $7 \times 10^{-5}$ M and [Co complex] = $2 \times 10^{-4}$ M.


dx.doi.org/10.1021/ic4016228 | *Inorg. Chem.* 2013, 52, 12535−12544

parameter, which indicates the hydrophobic character of molecules and their ability to cross lipid bilayers.[4,31] The calculated log P values for complexes **1**−**5** are −1.99, −2.18, −1.37, −2.45, −2.40, respectively. Complex **3** has the highest log P value and therefore the highest hydrophobicity, because of the four methyl groups on each diimine ligand, whereas complexes **1** and **2** with two methyl groups in each diimine ligand have intermediate values for log P and therefore moderate hydrophobicity. Complexes **4** and **5** with one methyl group in each diimine ligand have the lowest hydrophobicity.

**Cytotoxicity of Co-Complexes.** Cellular uptake and cytotoxicity of complexes **1**−**5** at low concentrations were assessed by flow cytometry on prostate cancer PC-3 cells, while their effects on intracellular mitochondrial function were measured by the MTS assay on HeLa and PC-3 cell lines. The cytotoxicity of our Co(III) phenanthroline complexes mediated by their effects on intracellular mitochondrial function was compared with that of a corresponding unsubstituted Co(III) complex[27] under similar conditions. $IC_{50}$ values indicate that each of the complexes **1**−**5** exhibits significantly higher cytotoxicity than the unsubstituted phenanthroline complex, (Table 2). Complex **3** has the highest

**Table 2. In-Vitro Cytotoxicity MTS Assay for Complexes 1−5 on PC-3 Cell Lines and for Other Reported Cobalt Complexes on Different Cancer Cell Lines**

| complex | cell lines | $IC_{50}$ values ± SD, $\mu$M | ref |
|---|---|---|---|
| $[Co(5,6\text{-dmp})_2Cl_2]Cl$ (**1**) | PC-3 | 2.71 ± 0.10 | present work |
| $[Co(4,7\text{-dmp})_2Cl_2]Cl$ (**2**) | PC-3 | 3.59 ± 0.29 | present work |
| $[Co(tmp)_2Cl_2]Cl$ (**3**) | PC-3 | 0.28 ± 0.08 | present work |
| $[Co(5\text{-mp})_2Cl_2]Cl$ (**4**) | PC-3 | 2.65 ± 0.06 | present work |
| $[Co(4\text{-mp})_2Cl_2]Cl$ (**5**) | PC-3 | 4.80 ± 0.76 | present work |
| $[Co(phen)_2Cl_2]Cl$ (ref) | PC-3 | 22.90 ± 1.41 | present work |
| Co-ASS | MCF-7 | 1.4 ± 0.3 | 38 |
| cisplatin | MCF-7 | 2.0 ± 0.3 | 38 |
| Co-ASS | MDA-MB | 1.9 ± 0.3 | 38 |
| cisplatin | MDA-MB | 4.0 ± 1.5 | 38 |
| rac-$[Co(phen)_3](ClO_4)_2$ | MCF-7 | 30.0 ± 1.0 | 23 |
| rac-$[Co(5,6\text{-dmp})_3](ClO_4)_2$ | MCF-7 | 20.0 ± 0.9 | 23 |

$IC_{50}$ value, 10 times higher than cisplatin, and 100 times higher than the unsubstituted Co-phenanthroline complex, whereas complexes **1**, **2**, **4**, and **5** have anticancer activities that are similar to those previously reported for cobalt and other metal complexes.[21−25,36−38] Interestingly, PC-3 cells were more affected by our methyl substituted phenanthroline Co(III) complexes than were HeLa cells, a result that indicates selective cytotoxicity disturbing the intracellular mitochondrial function (Supporting Information Table S6). Similar cell specific anticancer activity has been reported for other families of metal complexes.[31,39]

Generally, the uptake of nonfluorescent metal complexes in cells is examined by ICP-MS, AAS, and UV−vis.[39−43] However, these methods mainly use cell lysates for analysis, and these may not be representative of the actual cellular system. Therefore, in the present work we have studied cellular uptake and cytotoxicity of Co(III) complexes **1**−**5** by flow cytometry, which is well-known to provide more reliable and biologically relevant conditions, although the uptake cannot be quantified for nonfluorescent complexes.[32] Forward scattering (FS) provides information on the size of cells, while sideward scattering (SS) reflects the granularity and mass of the cells.[32,44] Thus SS allows the presence of a metal complex in cells to be determined, which is particularly important for nonfluorescent complexes.

Compared to control cells, complexes **1**−**5** all induced a shift toward slightly higher SS intensity, which indicates their uptake by the cells (Figure 8). The presence of complexes **1**−**5** inside the cells increased the scattered light compared to control cells, as detected in the high angle region. Additionally, higher SS intensity corresponds to an increase in the mass of the cells as a result of the complex uptake. The FS intensity of complexes **1**−**5** provides information regarding changes in the morphology and size of cells that can be correlated with cell death. Complex **2** induced a dramatic decrease in FS intensity; a slightly smaller effect was observed for complex **1**, while only a very small decrease in the FS was observed for complexes **4** and **5**. Thus complexes **2** and **1** affected the size and morphology of cells, whereas complexes **3**, **4**, and **5** affected them only slightly (Figure 8).

In order to quantify the cytotoxicity of our complexes in PC-3 cells when administrated in low amounts, we used propidium iodide (PI), a membrane-impermeable dye, and calculated the percentage of cell deaths based on a change in PI fluorescence. PI can enter into cells and bind to the nucleus only when the cell membrane is damaged, and this is thus correlated with cytotoxicity.[40] In PI staining assay, complex **2** showed the highest cytotoxicity (38%), followed by complex **1** (28%), while complexes **3**−**5** and the unsubstituted Co(III)complex[27] had a significantly lower cytotoxicity (11%, 7%, 6%, and 5%, respectively). The order of cytotoxicity level exhibited by complexes **1**−**5** obtained from flow cytometry data (**2** > **1** > **3** > **4** > ref > **5**) is different from that derived from the MTS assay data. This is not unexpected, because the cytotoxicity in the MTS assay is due to inhibition of mitochondrial function (resulting in a metabolic dysfunction), while in flow cytometry it is based on the level of PI permeability, which corresponds to the cell membrane damage, and is related to cell death. Although the MTS assay is commonly used for cytotoxicity assessment, recently it has been shown that the PI staining method is more sensitive for large cell populations, particularly at low concentrations of compounds.[45] In the case of our complexes, PI staining analysis indicates complementary cytotoxic behavior: complex **2** is the most cytotoxic, inducing cell membrane damage and therefore cell death, while complex **3** is more efficient in affecting the intracellular mitochondrial function, but only upon uptake. As any active compound that comes into contact with a cell first encounters its membrane, it is essential to assess the corresponding cytotoxic effect via the PI staining method, in addition to the MTS assay.

Cytotoxicity of metal complexes is associated with specific molecular factors, as for example the interaction with DNA[27] or their hydrophobicity and ability to cross lipid bilayers.[4,31] As the combination of CD, UV−vis spectroscopy titration, and EthBr displacement assay indicated only a weak DNA interaction for our complexes (the highest active complexes did not affect the DNA conformation), we investigated whether their hydrophobicity can be related to their cytotoxicity. Earlier studies suggested that there is a relationship between the hydrophobicity of phenanthroline based metal complexes and their


dx.doi.org/10.1021/ic4016228 | Inorg. Chem. 2013, 52, 12535−12544

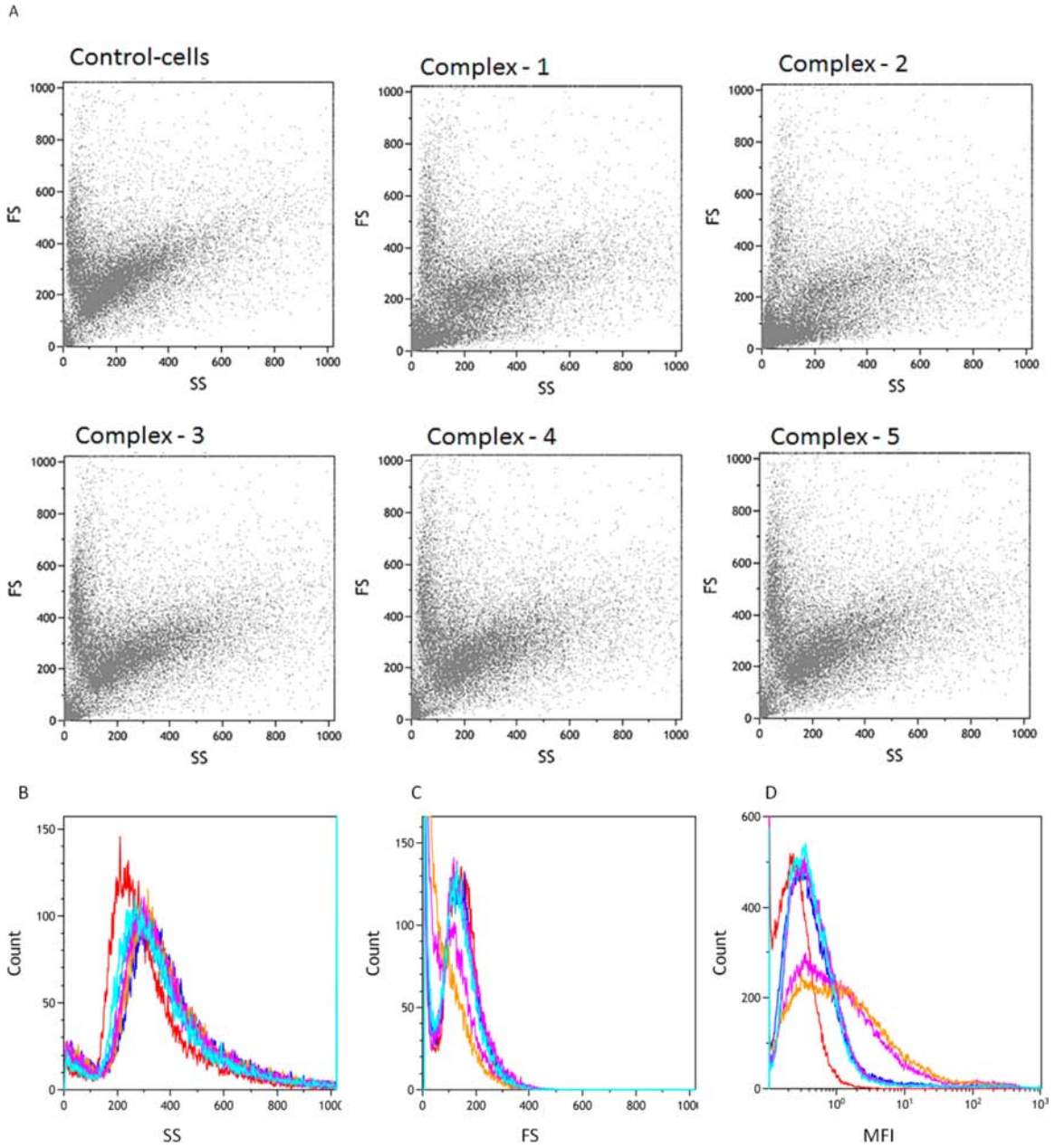


**Figure 8.** Flow cytometry analysis of PC-3 cells (control) and PC-3 cells treated with complexes **1**−**5**. (A) Density plot of FS vs SS; (B) histogram of SS intensity; (C) histogram of FS intensity; (D) in vitro toxicity assay of complexes **1**−**5** resulting from PI staining after 24 h.

level of cytotoxicity: an appropriate range of hydrophobicity values was necessary for high cytotoxicity, while too high or too low values decreased the biological effect.[31,46] Similarly, in the case of our Co(III)-complexes, the high cytotoxicity of complex **2** is mainly associated with a moderate hydrophobicity, while the higher hydrophobicity of complex **3**, is associated with a significantly decreased cytotoxicity (11%), as already reported for other metal complexes (Figure 9).[31,46] Complexes **4** and **5**, with a lower hydrophobicity than the other complexes, possess only minimal cytotoxicity (7% and 5%). These results indicate hydrophobicity that is too high or too low affects the ability of complexes to cross the cell membrane either by strongly interacting with it, or alternatively by avoiding any interaction. Thus, in our complexes hydrophobicity represents the molecular factor that modulates their cytotoxicity as obtained by PI staining method. Bell-shaped effects of hydrophobicity on cytotoxicity have been reported previously for other families of metal complexes.[31,46]

Our results indicate that molecular properties, such as hydrophobicity, are complementary to the interaction with DNA, which has been previously regarded as the main factor explaining the cytotoxicity of Co complexes. This is in agreement with other studies, which have also indicated alternative factors and mechanisms of metal complexes cytotoxicity, as for example interaction with proteins or induction of reactive oxygen species (ROS).[47−49] Detailed studies to address the mechanism of cytotoxicity of these Co complexes are ongoing.

## ■ CONCLUSION

We have described the synthesis of five new water-soluble Co(III) complexes with methyl substituted phenanthroline


dx.doi.org/10.1021/ic4016228 | Inorg. Chem. 2013, 52, 12535−12544

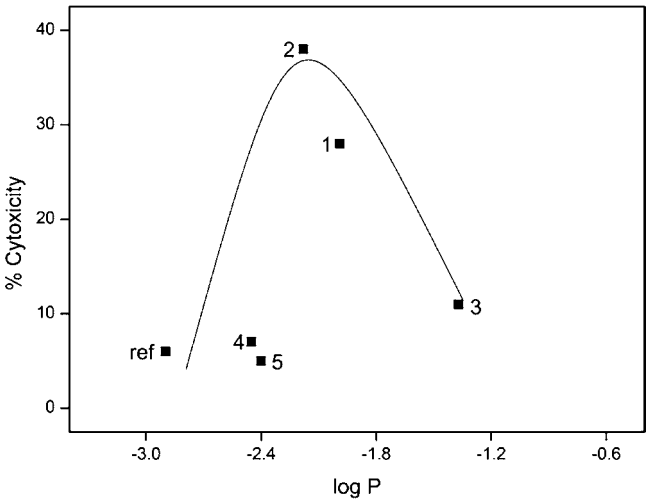


**Figure 9.** Cytotoxicity of complexes **1**−**5** as a function of their partition coefficient (log P).

ligands and tested their anticancer properties. Although the geometry of the metal coordination sphere changed only slightly from one complex to another, their hydrophobicity was strongly influenced by the position and numbers of methyl groups present in the ligands. A combination of CD, UV−vis spectroscopy titration, and EthBr displacement assay indicated that these complexes do not strongly interact with DNA, the proposed mechanism for action of anticancer platinum complexes. Antitumor activity of the new complexes was assessed by the MTS assay and flow cytometry. The significantly higher effects of complexes on intracellular mitochondrial function of PC-3 cells than of HeLa cells, as measured by the MTS assay, provides evidence for selective cytotoxicity. Cellular uptake and cytotoxicity of the complexes at low concentrations assessed by flow cytometry on PC-3 cells indicated that complex **2** was the most active, inducing around 38% cell death, whereas the other complexes had moderate cellular membrane-related cytotoxicity. The correlation between hydrophobicity of these cobalt complexes and their cytotoxicity demonstrated an important factor in antitumor activity, namely, a requirement for an appropriate hydrophobicity to facilitate the crossing of the cell membrane, which of necessity precedes cell death.

## ■ ASSOCIATED CONTENT

### Supporting Information

Crystallographic information and experimental details for Co(III) complexes. This material is available free of charge via the Internet at http://pubs.acs.org. CIF files for compounds **1** (CCDC 929966), **2** (CCDC 929964 and CCDC 929965), and **3** (CCDC 929967) have been deposited with the Cambridge Crystallographic Data Centre. Copies of data can be obtained, free of charge, on application to CCDC, 12 Union Road, Cambridge CB2 1EZ, U.K. (deposit@ccdc.com.ac.uk).

## ■ AUTHOR INFORMATION

### Corresponding Author

*E-mail: cornelia.palivan@unibas.ch. Fax: +41 (0)61267 3855. Tel: +41 (0) 61267 3839.

### Notes

The authors declare no competing financial interest.

## ■ ACKNOWLEDGMENTS

Financial support was provided by the University of Basel and the Swiss Federal Commission for Foreign Students Scholarships (the fellowship of S.J.), and this is gratefully acknowledged. S.J. acknowledges the financial support from the University Grants Commission, New Delhi, (No.F.4-1/2006 (BSR)/7-22/2007 (BSR)). S.J. thanks Prof. S. Arunachalam (Bharathidasan University, TN, India) for support and useful discussions. S.J. thanks to Pascal Tanner and Dr. Ozana Fischer from the University of Basel for discussions. The authors thank Dr. B. A. Goodman for editing the manuscript and useful discussions.

## ■ REFERENCES

(1) Reedijk, J. *Proc. Natl. Acad. Sci. U. S. A.* **2003**, *100*, 3611−3616.
(2) Todd, R. C.; Lippard, S. J. *Metallomics* **2009**, *1*, 280−291.
(3) Wang, D.; Lippard, S. J. *Nat. Rev. Drug. Discovery* **2005**, *4*, 307−320.
(4) Arnesano, F.; Natile, G. *Coord. Chem. Rev.* **2009**, *253*, 2070−2081.
(5) Jordan, P.; Carmo-Fonseca, M. *Cell. Mol. Life Sci.* **2000**, *57*, 1229−1235.
(6) Rebillard, A.; Lagadic-Gossmann, D.; Dimanche-Boitrel, M.-T. *Curr. Med. Chem.* **2008**, *15*, 2656−2663.
(7) Garrido, N.; Pérez-Martos, A.; Faro, M.; Lou-Bonafonte, J.; Fernández-Silva, P.; Lopez-Perez, M.; Montoya, J.; Enriquez, J. *Biochem. J.* **2008**, *414*, 93−102.
(8) Wong, E.; Giandomenico, C. M. *Chem. Rev.* **1999**, *99*, 2451−2466.
(9) Li, J.; Sun, K.; Ni, L.; Wang, X.; Wang, D.; Zhang, J. *Toxicol. Appl. Pharmacol.* **2012**, *258*, 376−383.
(10) Provencio, M.; Sánchez, A.; Artal, A.; Torres, J. S.; de Castro, J.; Dómine, M.; Viñolas, N.; Pérez, F. *Clin. Transl. Oncol.* **2013**, 1−6.
(11) Mahnken, R. E.; Billadeau, M. A.; Nikonowicz, E. P.; Morrison, H. *J. Am. Chem. Soc.* **1992**, *114*, 9253−9265.
(12) Butler, J. S.; Woods, J. A.; Farrer, N. J.; Newton, M. E.; Sadler, P. J. *J. Am. Chem. Soc.* **2012**, *134*, 16508−16511.
(13) Pierroz, V.; Joshi, T.; Leonidova, A.; Mari, C.; Schur, J.; Ott, I.; Spiccia, L.; Ferrari, S.; Gasser, G. *J. Am. Chem. Soc.* **2012**, *134*, 20376−20387.
(14) Cao, R.; Jia, J.; Ma, X.; Zhou, M.; Fei, H. *J. Med. Chem.* **2013**, *56*, 3636−44.
(15) Niyazi, H.; Hall, J. P.; O'Sullivan, K.; Winter, G.; Sorensen, T.; Kelly, J. M.; Cardin, C. J. *Nat. Chem.* **2012**, *4*, 621−628.
(16) Adsule, S.; Barve, V.; Chen, D.; Ahmed, F.; Dou, Q. P.; Padhye, S.; Sarkar, F. H. *J. Med. Chem.* **2006**, *49*, 7242−7246.
(17) Wheate, N. J.; Walker, S.; Craig, G. E.; Oun, R. *Dalton Trans.* **2010**, *39*, 8113−8127.
(18) Boulikas, T.; Pantos, A.; Bellis, E.; Christofis, P. *Cancer Ther.* **2007**, *5*, 537−583.
(19) Saha, D. K.; Sandbhor, U.; Shirisha, K.; Padhye, S.; Deobagkar, D.; Anson, C. E.; Powell, A. K. *Bioorg. Med. Chem. Lett.* **2004**, *14*, 3027−3032.
(20) Coyle, B.; Kinsella, P.; McCann, M.; Devereux, M.; O'Connor, R.; Clynes, M.; Kavanagh, K. *Toxicol. Vitro* **2004**, *18*, 63−70.
(21) Kemp, S.; Wheate, N. J.; Pisani, M. J.; Aldrich-Wright, J. R. *J. Med. Chem.* **2008**, *51*, 2787−2794.
(22) Ramakrishnan, S.; Suresh, E.; Riyasdeen, A.; Akbarsha, M. A.; Palaniandavar, M. *Dalton Trans.* **2011**, *40*, 3524−3536.
(23) Ramakrishnan, S.; Suresh, E.; Riyasdeen, A.; Akbarsha, M. A.; Palaniandavar, M. *Dalton Trans.* **2011**, *40*, 3245−3256.
(24) Rajendiran, V.; Karthik, R.; Palaniandavar, M.; Periasamy, V. S.; Akbarsha, M. A.; Srinag, B. S.; Krishnamurthy, H. *Inorg. Chem.* **2007**, *46*, 8208−8221.
(25) Ramakrishnan, S.; Shakthipriya, D.; Suresh, E.; Periasamy, V. S.; Akbarsha, M. A.; Palaniandavar, M. *Inorg. Chem.* **2011**, *50*, 6458−6471.

(26) Battaglia, V.; Compagnone, A.; Bandino, A.; Bragadin, M.; Rossi, C. A.; Zanetti, F.; Colombatto, S.; Grillo, M. A.; Toninello, A. *Int. J. Biochem. Cell Biol.* **2009**, *41*, 586−594.
(27) Ghosh, S.; Barve, A. C.; Kumbhar, A. A.; Kumbhar, A. S.; Puranik, V. G.; Datar, P. A.; Sonawane, U. B.; Joshi, R. R. *J. Inorg. Biochem.* **2006**, *100*, 331−343.
(28) Altomare, A.; Cascarano, G.; Giacovazzo, C.; Guagliardi, A.; Burla, M.; Polidori, G. t.; Camalli, M. *J. Appl. Crystallogr.* **1994**, *27*, 435−436.
(29) Farrugia, L. J. *J. Appl. Crystallogr.* **1997**, *30*, 565−565.
(30) Macrae, C. F.; Bruno, I. J.; Chisholm, J. A.; Edgington, P. R.; Mccabe, P.; Pidcock, E.; Rodriguez-Monge, L.; Taylor, R.; Streek, J. v.; Wood, P. A. *J. Appl. Crystallogr.* **2008**, *41*, 466−470.
(31) Aguirre, J. D.; Angeles-Boza, A. M.; Chouai, A.; Turro, C.; Pellois, J.-P.; Dunbar, K. R. *Dalton Trans.* **2009**, 10806−10812.
(32) Balasubramanian, V.; Onaca, O.; Ezhevskaya, M.; Van Doorslaer, S.; Sivasankaran, B.; Palivan, C. G. *Soft Matter* **2011**, *7*, 5595−5603.
(33) Jin, L.; Yang, P. *Polyhedron* **1997**, *16*, 3395−3398.
(34) Loganathan, R.; Ramakrishnan, S.; Suresh, E.; Riyasdeen, A.; Akbarsha, M. A.; Palaniandavar, M. *Inorg. Chem.* **2012**, *51*, 5512−5532.
(35) Ramakrishnan, S.; Palaniandavar, M. *Dalton Trans.* **2008**, 3866−3878.
(36) Lahiri, D.; Roy, S.; Saha, S.; Majumdar, R.; Dighe, R. R.; Chakravarty, A. R. *Dalton Trans.* **2010**, *39*, 1807−1816.
(37) Geldmacher, Y.; Kitanovic, I.; Alborzinia, H.; Bergerhoff, K.; Rubbiani, R.; Wefelmeier, P.; Prokop, A.; Gust, R.; Ott, I.; Wolfl, S.; Sheldrick, W. S. *ChemMedChem* **2011**, *6*, 429−439.
(38) Ott, I.; Schmidt, K.; Kircher, B.; Schumacher, P.; Wiglenda, T.; Gust, R. *J. Med. Chem.* **2005**, *48*, 622−629.
(39) Komor, A. C.; Schneider, C. J.; Weidmann, A. G.; Barton, J. K. *J. Am. Chem. Soc.* **2012**, *134*, 19223−19233.
(40) Puckett, C. A.; Ernst, R. J.; Barton, J. K. *Dalton Trans.* **2010**, *39*, 1159−70.
(41) Kirin, S. I.; Ott, I.; Gust, R.; Mier, W.; Weyhermüller, T.; Metzler-Nolte, N. *Angew. Chem., Int. Ed.* **2008**, *47*, 955−959.
(42) Egger, A. E.; Rappel, C.; Jakupec, M. A.; Hartinger, C. G.; Heffeter, P.; Keppler, B. K. *J. Anal. At. Spectrom.* **2009**, *24*, 51−61.
(43) Ghezzi, A.; Aceto, M.; Cassino, C.; Gabano, E.; Osella, D. *J. Inorg. Biochem.* **2004**, *98*, 73−78.
(44) Zucker, R.; Massaro, E.; Sanders, K.; Degn, L.; Boyes, W. *Cytometry Part A* **2010**, *77*, 677−685.
(45) Liao, T. T.; Jia, R. W.; Shi, Y. L.; Jia, J. W.; Wang, L.; Chua, H. *J. Environ. Sci. Health, Part A: Toxic/Hazard. Subst. Environ. Eng.* **2011**, *46*, 1769−1775.
(46) Aguirre, J. D.; Angeles-Boza, A. M.; Chouai, A.; Pellois, J.-P.; Turro, C.; Dunbar, K. R. *J. Am. Chem. Soc.* **2009**, *131*, 11353−11360.
(47) Tan, C.; Lai, S.; Wu, S.; Hu, S.; Zhou, L.; Chen, Y.; Wang, M.; Zhu, Y.; Lian, W.; Peng, W. *J. Med. Chem.* **2010**, *53*, 7613−7624.
(48) Pelosi, G. *Open Crystallogr. J.* **2010**, *3*, 16−28.
(49) Florea, A.-M.; Büsselberg, D. *Cancers* **2011**, *3*, 1351−1371.